IEEE Access
Multidisciplinary : Rapid Review : Open Access Journal

Received 16 August 2024, accepted 28 August 2024, date of publication 30 August 2024, date of current version 10 September 2024.
Digital Object Identifier 10.1109/ACCESS.2024.3452506

RESEARCH ARTICLE

# A Unit Commitment Model Considering the Flexibility Retrofit of Combined Heat and Power Units for Wind Integration

LEI YOU, XIAOMING JIN, AND YUN LIU
China Energy Engineering Group, Guangdong Electric Power Design Institute Company Ltd., Guangzhou, Guangdong 510663, China
Corresponding author: Lei You (youlei4031184@outlook.com)

This work was supported by the Science and Technology Project of China Energy Engineering Group Guangdong Electric Power Design Institute Company Ltd., under Grant EV11031W.

**ABSTRACT** In northern China, the combined heat and power (CHP) units account for a large proportion of the local generation capacity. However, the inherent heat-power coupling of CHP units poses a large barrier for wind power accommodation. To facilitate the local wind integration, the key is to improve the flexibility of the CHP system, and there are two types of feasible methods. One is the addition of heat storage tanks and electric boilers into the CHP system, and this method has been considered in the scheduling of the CHP system, such as the unit commitment (UC) optimization. The other type of method is the flexibility retrofit of CHP units, including the two-stage bypass modification and low-pressure cylinder removal (LPCR). However, prior research has not attempted to integrate the flexibility retrofit into the UC scheduling. To fill this gap, this paper proposes a novel UC model incorporating the bypass and LPCR retrofit of CHP units. In this model, the constraints on the safe operation region, fuel cost, reserve provision, ramping and mode switching of different types of CHP units are thoroughly described. Cases studies are conducted on a test system. Simulation results show that the proposed UC model is capable of utilizing the bypass and LPCR retrofit to facilitate wind accommodation, with the wind curtailment reduced by 81.94% and 20.45% under the bypass and LPCR retrofit, respectively.

**INDEX TERMS** Unit commitment (UC), combined heat and power (CHP) units, flexibility retrofit, two-stage bypass modification, low-pressure cylinder removal (LPCR).

## ABBREVIATIONS

| | |
|---|---|
| CHP | Combined heat and power. |
| HPC | High-pressure cylinder. |
| IPC | Intermediate-pressure cylinder. |
| LPC | Low-pressure cylinder. |
| LPCR | Low-pressure cylinder removal. |
| UC | Unit commitment. |
| HPB | High-pressure bypass. |
| LPB | Low-pressure bypass. |

## NOMENCLATURE

### SET AND INDICES

| | |
|---|---|
| $\mathcal{G}$ | Set of all thermal units, indexed by $g$. |
| $\mathcal{G}^C$, $\mathcal{G}^H$ | Sets of condensing units and CHP units, respectively. |
| $\mathcal{G}^{HB}$ | Set of CHP units with bypass retrofit. |
| $\mathcal{G}^{HL}$ | Set of CHP units with LPCR retrofit. |
| $\mathcal{R}$ | Set of wind farms, indexed by $r$. |
| $\mathcal{T}$ | Set of dispatch periods, indexed by $t$. |
| $\kappa$ | Set of heating districts, indexed by $k$. |
| $\mathcal{G}_k^H$ | Set of the CHP units providing heat to district $k$. |
| $\Omega$ | Set of all decision variables in unit commitment. |

### PARAMETERS

| | |
|---|---|
| $(Q_{gi}^j, P_{gi}^j)$ | Coordinate of the $i_{th}$ corner point in the $j_{th}$ sub-region of the safe operation region of CHP unit $g$. |

The associate editor coordinating the review of this manuscript and approving it for publication was R. K. Saket.

| | |
|---|---|
| $N_g^j$ | Number of corner points in the $j_{th}$ sub-region of the safe operation region of CHP unit $g$. |
| $k_g^{XY}$, $b_g^{XY}$ | Slope and intercept of the line from point X to point Y in the safe operation region of CHP unit $g$, respectively. |
| $\overline{R}_g^+/\overline{R}_g^-$ | Upper limit on the up-/down-reserve of thermal unit $g$. |
| $O_g^+/O_g^-$ | Up-/down-ramping limit of thermal unit $g$. |
| $\Delta t$ | Time interval of one dispatch step. |
| $(Q_g^X, P_g^X)$ | Heat and power output at point X in the safe operation region of CHP unit $g$. |
| $a_g/b_g$ | Coefficients for the variable/fixed fuel cost of thermal unit $g$. |
| $M$ | A sufficiently large positive number. |
| $\eta$ | Efficiency of bypass system. |
| $d_g^j$, $b_g^j$, $c_g^j$ | Coefficients in the general expression for the pure-power state of CHP unit $g$. |
| $T_g^+/T_g^-$ | Minimum time periods for the link valve of CHP unit $g$ to keep being closed/opened. |
| $C_g^U$ | Start-up cost of thermal unit $g$. |
| $C^{RC}$ | Cost for wind curtailment per MWh. |
| $C^{LS}$ | Cost for load shedding per MWh. |
| $T_g^U/T_g^D$ | Minimum on/off time of thermal unit $g$. |
| $\overline{P}_g/\underline{P}_g$ | Maximum/minimum output of thermal unit $g$. |
| $P_{rt}^{RA}$ | Available wind power at wind farm $r$ in time $t$. |
| $P_t^{PL}$ | Power load in time $t$. |
| $Q_{tk}^L$ | Heat load in district $k$ in time $t$. |
| $\zeta^{L+}/\zeta^{L-}$ | Factor of the up-/down-reserve requirement related to system load. |
| $\zeta^{R+}/\zeta^{R-}$ | Factor of the up-/down-reserve requirement related to wind power. |

### BINARY VARIABLES

| | |
|---|---|
| $I_{gt}^O$ | Commitment indicator for thermal unit $g$ in time $t$. |
| $S_{gt}^U/S_{gt}^D$ | Start-up/shut-down indicator for thermal unit $g$ in time $t$. |
| $I_{gt}^j$ | Binary variable denoting if the operating point of CHP unit $g$ in time $t$ falls into the $j_{th}$ sub-area of its safe operation region. |
| $I_{gt}^D$ | Binary variable denoting if the heat output of CHP unit $g$ in time $t$ exceeds $Q_g^D$. |

### CONTINUOUS VARIABLES

| | |
|---|---|
| $Q_{gt}^H/P_{gt}^H$ | Heat/power output of CHP unit $g$ in time $t$. |
| $C_{gt}^H/C_{gt}^C$ | Fuel cost of CHP/condensing unit $g$ in time $t$. |
| $R_{gt}^+/R_{gt}^-$ | Available up-/down-reserve of thermal unit $g$ in time $t$. |
| $P_{gt}^X$ | Power output of CHP unit $g$ if it is operating at the state $X$ in time $t$. |
| $\gamma_{git}^j$ | Combination coefficient for the $i_{th}$ corner point in the $j_{th}$ sub- region of the safe operation region of CHP unit $g$ in time $t$. |
| $w_{gt}^+/w_{gt}^-$ | Auxiliary variable denoting if the link valve of CHP unit $g$ is closed/opened in time $t$. |
| $P_{gt}^{Con}$ | Power output of condensing unit $g$ in time $t$. |
| $P_{rt}^{RO}/P_{rt}^{RC}$ | Dispatch output/wind curtailment at wind farm $r$ in time $t$. |

## I. INTRODUCTION

### A. MOTIVATION

Combined heat and power (CHP) units are the major contributor for providing heat in many countries [1], [2], and these units also account for a large proportion of local thermal generation capacity [3], [4]. Simultaneously, massive wind power has been installed around the world [5]. Take the inner Mongolia in northern China as an example, the local installed capacity of wind power has reached 4.57 GW in 2022, with an annual growth rate of 27.0% from 2018 to 2022 [6]. However, the inflexible operation of CHP units poses a serios barrier for the accommodation of local wind power. This is because the heat and power output of CHP units are strongly coupled, which narrows their power adjustment ability [7], [8]. Under the strong heat-power coupling, CHP units have to cover a large portion of power demand in the periods of high heat demand. Correspondingly, the room for renewable integration shrinks and the CHP system may need to curtail large renewable power for the sake of power balance.

Flexibility improvement of the CHP system is an important way to facilitate the wind power integration in northern China. Currently, there are mainly two types of methods for the flexibility enhancement. The first method relies on the integration of heat-power decoupling devices into the CHP system, which mainly include the heat storage tanks (see [9], [10]) and electric boiler (see [11], [12]). The second type of method utilizes the flexibility retrofit of CHP units themselves, such as the two-stage bypass modification (see [7], [13]) and low-pressure cylinder removal (LPCR) (see [12], [14], [15]).

This paper focuses on the flexibility retrofit of CHP units. Particularly, it is noticed that the previous scheduling models of the CHP system have not considered the flexibility retrofit of CHP units yet, such as the unit commitment (UC) scheduling. It motivates this paper to develop an effective and tractable UC model which can incorporate the flexibility retrofit of CHP units.

### B. LITERATURE REVIEW

Some research has been carried out to study the effects of the flexibility improvement methods on accommodating renewable power. The work in [7] compares the heat storage tanks, electric boilers, two-stage bypass and LPCR in terms of their capability in facilitating wind absorption, and the results show that the electric boilers and bypass have the overall best performance. Similarly, the efficiency of electric boilers and bypass modification in improving renewable consumption is also highlighted in [16]. The study in [13] builds a series of mathematical models to analyze the wind accommodation ability of the CHP units under different flexibility improvement methods, and it is found that the CHP units with two-stage bypass have the best capability while it is the worst with heat storage tank. Reference [17] proposes a novel CHP system integrated with various flexible technologies, and the simulation reveals the ability of heat storage and LPCR in facilitating the wind power integration. Reference [18] focuses on the flexibility retrofit of CHP units and the quantitative analyses show that, compared to the high back-pressure retrofit, the LPCR retrofit presents greater potential to improve the renewable accommodation. In summary, the prior work in the literature has showed that various flexibility improvement methods are effective in improving the renewable integration in the CHP system.

Meanwhile, some prior studies have attempted to integrate the flexibility improvement into the operational scheduling of the CHP system. The heat storage and electric boiler have been considered in the centralized dispatch of the CHP system [19]. These two devices have been also incorporated into the UC optimization of the CHP system, see [20]. Further, [3] investigated how to combine the flexibility of heat storages with the improved modelling of ramping and reserve constraints in UC. The electric boiler is also utilized in the economic dispatch of the CHP system to accommodate wind power [21]. Besides, an integrated UC and economic dispatch model for the CHP system is established in [22], which leverages the flexibility of heat storages and electric boilers to reduce the wind and solar curtailment. In reference [4], the renovation based on the internal and external thermal storages is applied to CHP units and included in the UC modelling of the CHP system.

The above discussions show that some UC models have already considered the flexibility improvement of the CHP system, but they only focus on the application of heat storages and electric boilers. To be contrary, the two-stage bypass modification and LPCR are two typical technologies for the flexibility retrofit of CHP units, but they have not been integrated into the UC optimization of the CHP system. Either, it is not clear how to model these two retrofit techniques in the UC modelling.

### C. CONTRIBUTIONS

To fill the aforementioned gaps in the literature, this paper proposes a novel UC model which explicitly accounts for the two-stage bypass and LPCR of CHP units. In this model, the operation of the CHP unit without and with flexibility retrofit is thoroughly modelled based on the operational characteristics and retrofit principles of CHP units. The modelling of the CHP units involves their safe operation regions, fuel cost, ramping capability, reserve capacities and mode switching. The effectiveness of the proposed UC model is also verified by case studies.

The work in this paper has the following contributions:

- In this paper, the operation of the CHP units with two-stage bypass and LPCR is modelled through tractable formulation, which can be readily integrated into the UC modelling. In the formulation, the constraints on the safe operation region, operating cost, ramping, reserve provision and mode switching of the CHP units are described in detail. Such formulation enriches the understanding on how to model the operation of CHP units with flexibility retrofit.
- This paper proposes a novel UC model which can incorporate the bypass and LPCR retrofit of CHP units. This UC model fills the gap in the literature that the existing relevant UC models have not attempted to utilize the two-stage bypass and LPCR. The proposed UC model can be used to release the hidden flexibility of CHP units, enabling the integration of more wind power in the day-ahead dispatch of the CHP system.
- Case studies show that the proposed UC model can effectively exploit the flexibility from the bypass and LPCR retrofit to facilitate wind accommodation. Numerical tests also compare the capability of bypass system and LPCR in improving wind integration.

### D. ORGANIZATION OF THE PAPER

This paper is structured as follows. Section II presents how to model the operation of different types of CHP units. Section III gives the full formulation of the proposed UC model. Section IV conducts case studies. Section V concludes the paper.

## II. MODELLING OF THE OPERATION OF CHP UNITS

This section models the operation of different types of CHP units, which involves the safe operation region, fuel cost, ramping, reserve provision and mode switching of the units. Here, the CHP units are categorized into the ones without flexibility retrofit, the ones with bypass retrofit and the ones with LPCR retrofit.

### A. OPERATION OF CHP UNITS WITHOUT FLEXIBILITY RETROFIT

The extraction-type CHP unit is widely applied in China, and it generally consists of high pressure cylinder (HPC), intermediate pressure cylinder (IPC), low pressure cylinder (LPC) and other mechanical components [7]. The operational principle of the extraction-type CHP unit is shown in Fig. 1. It is seen that part of the exhaust steam from the IPC enters the LPC to generate power, while the other part enters the heating network to produce heat. In practice, a CHP unit can adjust the inlet steam flow rate of the LPC by controlling the extraction valve and link valve, thus regulating both the power and heat output of the unit.

#### 1) SAFE OPERATION REGION

In [7], a typical CHP unit in northern China is taken as the research object, and it is found that the safe operation region of the CHP unit can be described by a pentagon, see Fig. 2. This region is surrounded by five boundaries AB, BC, CD, DE and EA. Lines AB and ED represent the heat-power coupling curves under the maximum and minimum main

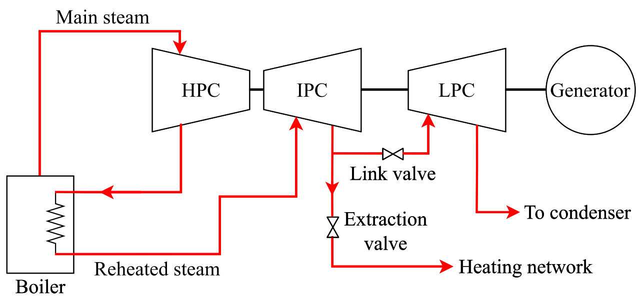


**FIGURE 1.** **Operational principle of extraction-type CHP unit.**

steam flow rates, respectively. Line AE denotes that the CHP unit operates in the pure-power (condensing) mode. Line BC depicts the operation curve under the maximum extraction rate of the heating steam, i.e., the heating output of the unit reaches its upper limit. On the line CD, the steam flow entering the LPC reaches the minimum required rate.

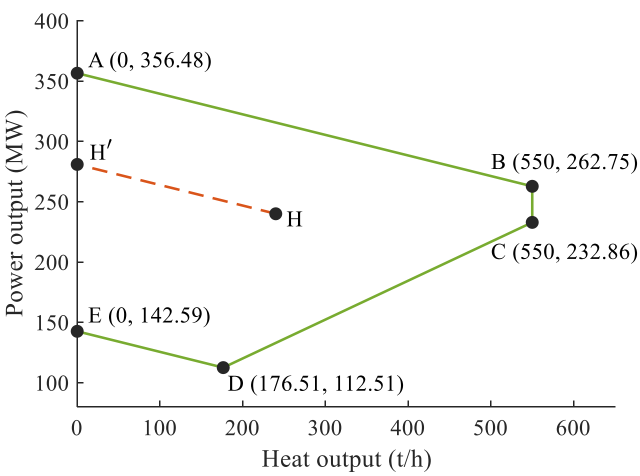


**FIGURE 2.** **Safe operation region of the CHP unit without flexibility retrofit.**

From Fig. 2, it is clear that the upper and lower limits on the power output of the CHP unit depends on its heat production. As the heat output increases and exceeds $Q_g^D$ (i.e., 176.51 t/h), the adjustment range of the power output becomes narrower, and the minimum allowable power output gradually increases. And in the periods with high heat load, the CHP unit has to maintain a high level of power output in order to meet the heat demand. As a result, the CHP system may not have sufficient room to accommodate all the renewable output.

Assuming that the CHP unit operates at the point H in Fig. 2, its heat output $Q_{gt}^H$ and power output $P_{gt}^H$ can be represented by a convex combination of the coordinates of the corner points A-E [20]. Mathematically, this can be expressed as:

$$Q_{gt}^H = \sum_{i=1}^{N_g^1} Q_{gi}^1 \gamma_{git}^1 \tag{1}$$

$$P_{gt}^H = \sum_{i=1}^{N_g^1} P_{gi}^1 \gamma_{git}^1 \tag{2}$$

$$\gamma_{git}^1 \geq 0, \forall i = 1, \cdots, N_g^1 \tag{3}$$

$$\sum_{i=1}^{N_g^1} \gamma_{git}^1 = I_{gt}^O \tag{4}$$

where $(Q_{gi}^1, P_{gi}^1)$ denotes the coordinate of the $i_{th}$ corner point.

### 2) RESERVE CAPACITIES

Through the adjustment of power production, CHP units can provide upward reserve $R_{gt}^+$ and downward reserve $R_{gt}^-$ to the CHP system. As shown in Fig. 2, the available $R_{gt}^+$ and $R_{gt}^-$ are related to the heat output of the unit, with $R_{gt}^+$ bounded by line AB and $R_{gt}^-$ bounded by lines ED and DC. Thus, the reserve capacities of the unit can be expressed by the following constraints:

$$P_{gt}^H + R_{gt}^+ \leq k_g^{AB} Q_{gt}^H + b_g^{AB} I_{gt}^O \tag{5}$$

$$P_{gt}^H - R_{gt}^- \geq k_g^{ED} Q_{gt}^H + b_g^{ED} I_{gt}^O \tag{6}$$

$$P_{gt}^H - R_{gt}^- \geq k_g^{DC} Q_{gt}^H + b_g^{DC} I_{gt}^O \tag{7}$$

$$0 \leq R_{gt}^+ \leq \overline{R}_{gt}^+ \tag{8}$$

$$0 \leq R_{gt}^- \leq \overline{R}_{gt}^- \tag{9}$$

where $k_g^{XY}$ and $b_g^{XY}$ denote the slope and intercept of the line connecting points $X$ and $Y$, respectively.

### 3) RAMPING LIMITS

The ramping limits of the CHP unit can be modelled based on its pure-power (condensing) state. To illustrate this point, line HH' is built and it is parallel to line AB, see Fig. 2. Point H' denotes the pure-power state corresponding to H, and the pure power at H' can be calculated by (10). As the operating state of the unit shifts from H' to H, less steam enters the LPC to produce power while more steam is extracted for heat production, but the main steam flow rate from the boiler remains constant. Meanwhile, for the sake of operational safety, the change rate in the main steam flow rate needs to be restricted. Since the CHP unit has the same main steam flow rates at states H and H,' the restriction on the main steam at H is equivalent to that at H.' This is further equivalent to restricting the ramping of the pure-power at H,' where all the main steam is used for power generation. Based on the above analysis, the following constraints can be developed to limit the change rate in the main steam flow under any working-state (pure-power or not).

$$P_{gt}^{H'} = P_{gt}^H - k_g^{AB} Q_{gt}^H \tag{10}$$

$$P_{gt}^{H'} - P_{g,t-1}^{H'} \leq I_{g,t-1} O_g^+ \Delta t + S_{gt}^U \max(O_g^+ \Delta t, P_g^E) \tag{11}$$

$$P_{g,t-1}^{H'} - P_{gt}^{H'} \leq I_{gt} O_g^- \Delta t + S_{gt}^D \max(O_g^- \Delta t, P_g^E) \tag{12}$$

where $P_{gt}^{H'}$ is the power output at the pure-power state; $P_g^X$ represents the power output at the operating point $X$ in Fig. 2.

#### 4) FUEL COST

Since the main steam flow rate of the CHP unit at state H is the same as that at state H,' the fuel cost at H is equal to that at H' and can be expressed by (13), where the right-hand side of the equation denotes the fuel cost of the CHP unit under pure-power state.

$$C_{gt}^{H} = a_g P_{gt}^{H'} + b_g I_{gt} \tag{13}$$

### B. OPERATION OF CHP UNITS WITH BYPASS RETROFIT

As for the bypass retrofit of CHP units, this paper focuses on the two-stage bypass modification since it has been carried out in northern China [23]. Actually, the two-stage bypass is advantageous in its high steam flow, high heating power and low overtemperature risk of the reheater [24].

The operational principle of the CHP unit with two-stage bypass is illustrated in Fig. 3 [7]. It can be observed that: 1) part of the main steam is desuperheated and depressurized by the high-pressure bypass (HPB), mixed with the exhaust steam from the HPC, and then enters the reheater; 2) part of the reheated steam is desuperheated and depressurized by the low-pressure bypass (LPB), mixed with the extraction steam from the IPC, and is then fed to the heating network heater.

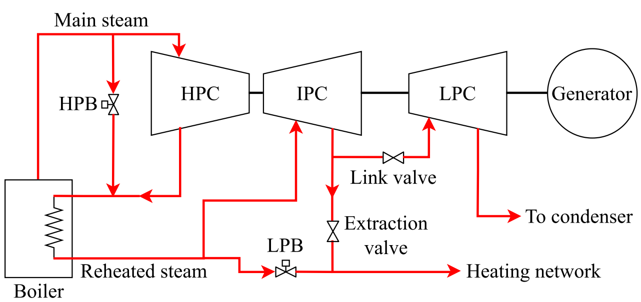


**FIGURE 3. Operational principle of extraction-type CHP unit with two-stage bypass.**

It should be noted that this paper focuses on the UC modelling and the impact of bypass retrofit on UC scheduling, rather than the design or dynamic simulation of bypass systems. The existing design of two-stage bypass from [7] is used in this paper since it is the typical representation of the bypass systems in northern China. As for the influence of the internal parameters (e.g., valve characteristics) on the bypass performance, readers can refer to [25] and [26].

#### 1) SAFE OPERATION REGION

After the bypass retrofit, the safe operation range of the CHP unit in Section II-A can be expanded from the area ABCDE to area ABFGDE (see Fig. 4 [7]), so its operational flexibility is enlarged. Particularly, for the periods with high heat load, the bypass-CHP unit can shift its operating point down below area ABCDE to further reduce its power output, providing larger room for renewable integration.

It is also shown in Fig. 4 that, different to area ABCDE, area ABFGDE is not a convex polygon. In order to model the heat-power output of the unit, area ABFGDE is divided into three convex sub-regions: ABCDE (sub-region 1), CKGD (sub-region 2) and BFKC (sub-region 3). Note that line CK is parallel to both lines BF and DG.

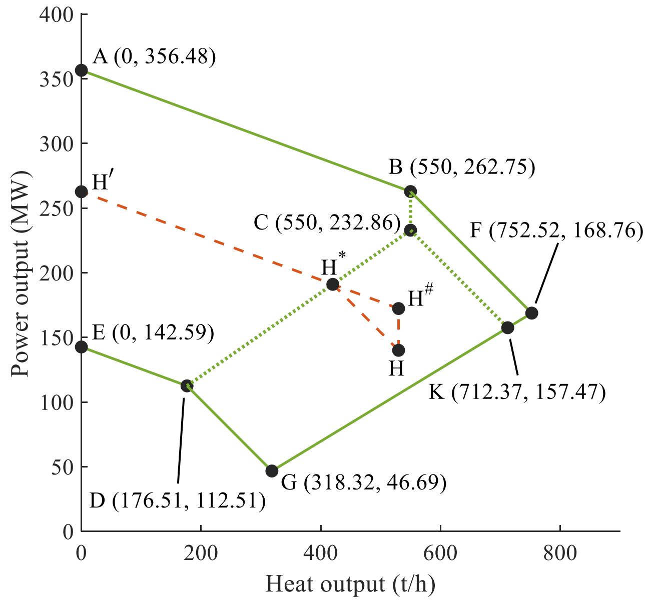


**FIGURE 4. Safe operation region of the CHP unit with bypass retrofit.**

Let $(Q_{gi}^{j}, P_{gi}^{j})$ denote the coordinate of the $i_{th}$ corner point in the $j_{th}$ sub-region, the heat output $Q_{gt}^{H}$ and power output $P_{gt}^{H}$ of the bypass-CHP unit can be expressed by the combination of the corner points in all sub-regions, as shown below.

$$Q_{gt}^{H} = \sum_{j=1}^{3} \sum_{i=1}^{N_g^j} Q_{gi}^{j} \gamma_{git}^{j} \tag{14}$$

$$P_{gt}^{H} = \sum_{j=1}^{3} \sum_{i=1}^{N_g^j} P_{gi}^{j} \gamma_{git}^{j} \tag{15}$$

$$\gamma_{git}^{j} \geq 0, \forall i = 1, \cdots, N_g^j, \forall j = 1, 2, 3 \tag{16}$$

$$\sum_{i=1}^{N_g^j} \gamma_{git}^{j} = I_{gt}^{j} \tag{17}$$

$$\sum_{j=1}^{3} I_{gt}^{j} = I_{gt}^{O} \tag{18}$$

Note that with (17)-(18), the CHP unit can operate in only one of the three sub-regions during any given time interval.

#### 2) RESERVE CAPACITIES

Depending on the heat output $Q_{gt}^{H}$, the upper power limit of the bypass-CHP unit is determined by line AB or BF, so the following constraints can be used to model the up-reserve capacity of the unit.

$$P_{gt}^{H} + R_{gt}^{+} \leq k_g^{AB} Q_{gt}^{H} + b_g^{AB} \tag{19}$$

$$P_{gt}^{H} + R_{gt}^{+} \leq k_g^{BF} Q_{gt}^{H} + b_g^{BF} \tag{20}$$

$$0 \leq R_{gt}^{+} \leq I_{gt}^{O}\overline{R}_{gt}^{+} \tag{21}$$

The lower power limit of the bypass-CHP unit is determined by lines ED, DG and GF. Note that lines ED and DG are intersected in a non-convex manner. To model the down-reserve capacity of the unit in a tractable way, a new binary variable $I_{gt}^{D}$ is introduced and it denotes if the heat output of the unit exceeds $Q_{g}^{D}$. With $I_{gt}^{D}$, the available down-reserve can be constrained by (22)-(27).

$$Q_{gt}^{H} \geq I_{gt}^{D}Q_{g}^{D} \tag{22}$$

$$P_{gt}^{H} - R_{gt}^{-} \geq k_{g}^{ED}Q_{gt}^{H} + b_{g}^{ED}I_{gt}^{O} - I_{gt}^{D}M \tag{23}$$

$$P_{gt}^{H} - R_{gt}^{-} \geq k_{g}^{DG}Q_{gt}^{H} + b_{g}^{DG}I_{gt}^{O} + \left(I_{gt}^{D} - 1\right)M \tag{24}$$

$$P_{gt}^{H} - R_{gt}^{-} \geq k_{g}^{GF}Q_{gt}^{H} + b_{g}^{GF}I_{gt}^{O} \tag{25}$$

$$0 \leq R_{gt}^{+} \leq \overline{R}_{gt}^{+} \tag{26}$$

$$0 \leq R_{gt}^{-} \leq \overline{R}_{g}^{-} \tag{27}$$

Specifically, if $Q_{gt}^{H} \leq Q_{g}^{D}$, constraint (22) will enforce $I_{gt}^{D} = 0$, and constraint (23) will be activated, with line ED bounding the down-reserve; if $Q_{g}^{D} < Q_{gts}^{H} \leq Q_{g}^{G}$, constraint (22) allows $I_{gt}^{D}$ to equal 1, so constraint (24) (i.e., line DG) can be activated to bound the down-reserve; similarly, if $Q_{gt}^{H}$ exceeds $Q_{g}^{G}$, $I_{gt}^{D}$ can take the value of 1 to activate (24), with the down-reserve bounded by line DG or GF (depending on $Q_{gt}^{H}$).

### 3) RAMPING LIMITS

Similar to the CHP unit without retrofit, the ramping capacity of the bypass-CHP unit can be modelled based on its pure-power state H.' The key is how to identify the pure-power at H' and express it in a tractable way.

a) If the operating point H of the unit is in area ABCDE, the unit is operating in the conventional extraction mode and the corresponding pure-power at H' can be expressed by constraint (10).

b) If H is in area CKGD, the bypass system is working and part of main steam is extracted for heat production. In this process, part of the available energy is lost since some high-grade steam is artificially converted into low-grade steam [7]. This is the result of the second law of thermodynamics. The lost energy $\Delta E$ can be estimated by the method in [7]:

$$\Delta E = D_1E_1 - D_2E_2 \tag{28}$$

$$E_1 = (h_1 - h_0) - T_0(S_1 - S_0) \tag{29}$$

$$E_2 = (h_2 - h_0) - T_0(S_2 - S_0) \tag{30}$$

where $D_1$, $E_1$, $h_1$ and $S_1$ are the flow rate, available energy, enthalpy, entropy of high-grade steam, respectively; $D_2$, $E_2$, $h_2$ and $S_2$ are the flow rate, available energy, enthalpy, entropy of low-grade steam, respectively; $h_0$, $T_0$ and $S_0$ are the steam enthalpy, steam temperature and steam entropy in environmental state, respectively.

If the energy loss is neglected, the operating state of the unit will be shift upward from H to H,$^{\#}$ as shown in Fig. 4. Clearly, H$^{\#}$ has the same heat output as H, but its power output is higher. Based on the coordinate of H,$^{\#}$ the pure-power point H' can be found, with H$^{\#}$H' parallel to AB. Moreover, H$^{\#}$H' and CD are intersected at point H.* To avoid confusion, the operating states denoted by points H,' H,*H$^{\#}$ and H are re-listed as below:

- H': the unit operates in the condensing mode and the bypass system is not working;
- H*: the inlet steam flow rate of LPC has reduced to the minimum limit and the bypass system is not working;
- H$^{\#}$: the bypass system is working and the energy loss is neglected;
- H: the bypass system is working.

From H* to H,$^{\#}$ a larger part of the main steam is extracted through the bypass system and used for heat generation. Also, the main steam flow rate of the unit remains constant at points H, H$^{\#}$ H*, and H.'

Besides, the relationship between the power outputs at points H, H* and H$^{\#}$ has been also studied in [7] and can be expressed by (31).

$$P_{gt}^{H} = P_{gt}^{H^*} - \frac{P_{gt}^{H^*} - P_{gt}^{H^\#}}{\eta} \tag{31}$$

where $\eta$ is the efficiency of bypass system and it can be derived based on the estimation of the energy loss $\Delta E$; the details to derive $\eta$ can refer to [7] and are not unfolded here; it should be noted that the bypass modification introduces additional dynamic elements (e.g., pressure changes), the influence of the dynamic factors on the bypass system performance can refer to [27] and [28] and is not the research focus of this paper.

Meanwhile, constraints (32)-(34) hold since H$^{\#}$ has the same heat output as H, line H* H$^{\#}$ is parallel to line AB and H* is on line CD, respectively.

$$Q_{gt}^{H^\#} = Q_{gt}^{H} \tag{32}$$

$$P_{gt}^{H^\#} - P_{gt}^{H^*} = k_{g}^{AB}(Q_{gt}^{H^\#} - Q_{gt}^{H^*}) \tag{33}$$

$$P_{gt}^{H^*} - P_{g}^{D} = k_{g}^{DC}(Q_{gt}^{H^*} - Q_{g}^{D}) \tag{34}$$

Based on the coordinate of H,* the pure power at H' can be expressed by the following constraint.

$$P_{gt}^{H'} = P_{gt}^{H^*} - k_{g}^{AB}Q_{gt}^{H^*} \tag{35}$$

By combining (31)-(35), it is easy to express the pure power at H' as a linear function of $P_{gt}^{H}$ and $Q_{gt}^{H}$, as shown below.

$$P_{gt}^{H'} = \frac{\eta(k_{g}^{AB} - k_{g}^{DC})}{k_{g}^{AB} - \eta k_{g}^{DC}}P_{gt}^{H} + \frac{k_{g}^{AB}(k_{g}^{DC} - k_{g}^{AB})}{k_{g}^{AB} - \eta k_{g}^{DC}}Q_{gt}^{H} + \frac{k_{g}^{AB}(1-\eta)(P_{g}^{D} - k_{g}^{DC}Q_{g}^{D})}{k_{g}^{AB} - \eta k_{g}^{DC}} \tag{36}$$

c) If H is in area BFKC, the pure-power state H' can be identified in the same principle as that when H falls in area CKGD. Two lines HH,$^{\#}$ H$^{\#}$H' can be also built, with H$^{\#}$H' parallel to AB. Thus, constraints (31)-(33) still take effects.

The only difference is that H* is located on line BC, i.e., constraint (37) holds. By combining (31)-(33), (35) and (37), the power output at H' can be identified through (38).

$$Q_{gt}^{H^*} = Q_g^B \tag{37}$$

$$P_{gt}^{H'} = P_{gt}^{H} - \frac{k_g^{AB}}{\eta} Q_{gt}^{H} + \frac{k_g^{AB} Q_g^B (1-\eta)}{\eta} \tag{38}$$

The above analysis shows that the expression of the pure-power $P_{gt}^{H'}$ depends on the area that H falls inside, but it can be written in the following general form:

$$P_{gt}^{H'} = a_g^j P_{gt}^{H} + b_g^j Q_{gt}^{H} + c_g^j \tag{39}$$

where the coefficients $a_g^j$, $b_g^j$ and $c_g^j$ depend on the area that H falls inside, and they can be easily extracted from (10), (36) and (38).

Further, by combining (14)-(17) and (39), the expressions for $P_{gt}^{H'}$ in different cases can be integrated into one single constraint, which is tractable for UC optimization:

$$P_{gt}^{H'} = \sum_{j=1}^{3} \left( a_g^j \sum_{i=1}^{N_g^j} P_{gi}^j \gamma_{git}^j + b_g^j \sum_{i=1}^{N_g^j} Q_{gi}^j \gamma_{git}^j + c_g^j I_{gt}^j \right) \tag{40}$$

Finally, the ramping constraints for the bypass-CHP unit can be constructed as (11)-(12) and (40).

#### 4) FUEL COST

Similar to the CHP units without retrofit, the fuel cost of the bypass-CHP unit can be expressed by (13).

### C. OPERATION OF CHP UNITS WITH LPCR RETROFIT

If the LPCR retrofit is applied to a CHP unit, the link valve of the unit can be closed to cut off nearly all the steam entering the LPC (see Fig. 5). This reduces the power output of the unit and allows more steam to enter the heating network through the extraction valve. As a result, the CHP unit can provide the same amount of heat with less power output. Note that after the LPCR retrofit, the power generation of the LPC can be switched between "non-zero" and "zero" by closing and opening the link valve. The design of the LPCR system from [7] is used in this paper and more technical details of LPCR can be also found in [7].

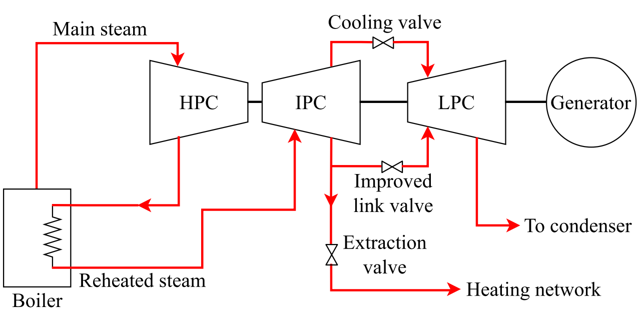


**FIGURE 5. Operational principle of extraction-type CHP unit with LPCR.**

#### 1) SAFE OPERATION REGION AND FUEL COST

Suppose the CHP unit in Section II-A completes the LPCR retrofit, its safe operation range will change, as shown in Fig. 6 [7]. This region can be divided into three sub-regions: area ABCDE (sub-region 1), line B'C' (sub-region 2) and line C'D' (sub-region 3). By closing and opening the link valve, the operation region can be switched back and forth between the area ABCDE and lines B'C'-C'D.' Note that the unit cannot operate in the areas BB'C'C and CC'D'D. By transferring the operating point to lines B'C'-C'D,' the unit can produce less power output while meeting the high heat load, leaving larger room for renewable integration. Also, the heating capability of the unit is enhanced.

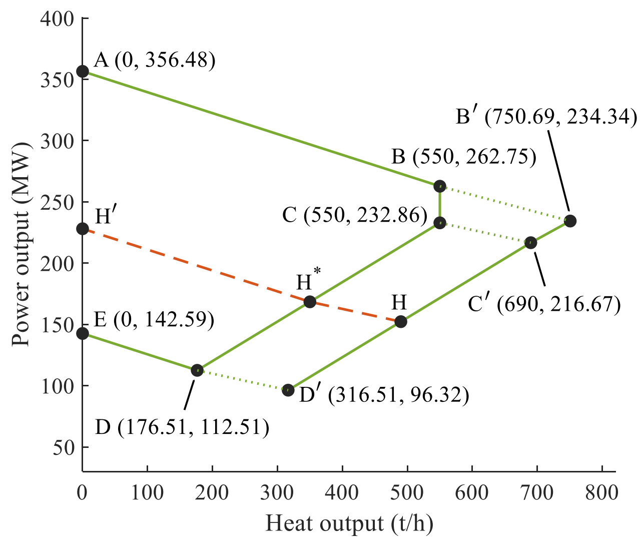


**FIGURE 6. Safe operation range of the CHP unit with LPCR retrofit.**

Same to the bypass-CHP unit, the heat and power output of the LPCR-CHP unit can be modelled by the combination of the coordinates in the sub-regions, see (14)-(18), and the fuel cost can be expressed by (13).

#### 2) RESERVE CAPACITIES

The LPCR-CHP unit can provide up- and down-reserve when it is operating in the sub-region ABCDE, with the up-reserve bounded by line AB and the down-reserve bounded by lines ED and DC. However, if the unit operates on the line B'C' or C'D,' the unit cannot adjust its power output under the given heat output, i.e., the unit has no reserve capacity. Based on the above analysis, the up- and down-reserve capacities of the LPCR-CHP unit can be modelled by constraints (41)-(45). With these constraints, the up-reserve $R_{gt}^+$ and down-reserve $R_{gt}^-$ can be non-zero only when $I_{gt}^1 = 1$, i.e., when the unit operates in the area ABCDE.

$$\sum_{i=1}^{N_g^1} P_{gi}^1 \gamma_{git}^1 + R_{gt}^+ \leq k_g^{AB} \sum_{i=1}^{N_g^1} Q_{gi}^1 \gamma_{git}^1 + b_g^{AB} I_{gt}^1 \tag{41}$$

$$\sum_{i=1}^{N_g^1} P_{gi}^1 \gamma_{git}^1 - R_{gt}^- \geq k_g^{ED} \sum_{i=1}^{N_g^1} Q_{gi}^1 \gamma_{git}^1 + b_g^{ED} I_{gt}^1 \quad (42)$$

$$\sum_{i=1}^{N_g^1} P_{gi}^1 \gamma_{git}^1 - R_{gt}^- \geq k_g^{DC} \sum_{i=1}^{N_g^1} Q_{gi}^1 \gamma_{git}^1 + b_g^{DC} I_{gt}^1 \quad (43)$$

$$0 \leq R_{gt}^+ \leq \overline{R}_g^+ \quad (44)$$

$$0 \leq R_{gt}^- \leq \overline{R}_g^- \quad (45)$$

### 3) RAMPING LIMITS

Similar to the bypass-CHP unit, the ramping limits of the LPCR -CHP unit can be modelled based on its pure-power state H.' The expression for the pure-power at H' depends on the sub-region that the operating point H falls at.

a) If H is in area ABCDE, the corresponding pure-power at H' can be expressed by constraint (10).

b) If H is located on line D'C,' there exists an operating point H* on line DC, and as the operating state of the unit shifts from H* to H (see Fig. 6), the link valve of the unit is closed and the steam flow entering the LPC reduces from the minimum required amount to nearly zero. Correspondingly, the power generation of the LPC turns from ''non-zero'' to ''zero'' and the steam flow for heating is increased. Reference [7] has provided the linear relationship between the power generation of the LPC and its inlet steam flow. This can be used to develop the relationship between the coordinates of H and H*:

$$P_{gt}^{H^*} - P_{gt}^{H} = k_g^R \left( Q_{gt}^{H} - Q_{gt}^{H^*} \right) - b_g^R \quad (46)$$

where $k_g^R$ and $b_g^R$ are fitting coefficients and their values are set to 0.2014 and 12.01 in [7], respectively.

Considering that point H* is located on the line DC, the following constraint also holds:

$$P_{gt}^{H^*} - P_g^D = k_g^{DC} \left( Q_{gt}^{H^*} - Q_g^D \right) \quad (47)$$

In addition, the coordinate of H* and the pure power at H' satisfy the relationship in (35). Thus, by combining (35) and (46)-(47), the pure power at H' can be expressed as a linear function of $Q_{gt}^H$ and $P_{gt}^H$, as shown below.

$$P_{gt}^{H'} = \frac{k_g^{DC} - k_g^{AB}}{k_g^{DC} + k_g^R} P_{gt}^H + \frac{k_g^R (k_g^{DC} - k_g^{AB})}{k_g^{DC} + k_g^R} Q_{gt}^H + \frac{\left(k_g^R + k_g^{AB}\right)\left(P_g^D - k_g^{DC} Q_g^D\right) - (k_g^{DC} - k_g^{AB}) b_g^R}{k_g^{DC} + k_g^R} \quad (48)$$

c) If H is located on line B'C,' there exists an operating point H* on line BC, and as the operating state of the unit is switched from H* to H, the link valve is closed. This is similar to the case when H is located on line D'C.' Thus, (46) can be still used to describe the relationship between the coordinates of H and H*. Meanwhile, it is obvious that the following constraint (49) holds since H* is located on line BC. By combining (35), (46) and (49), the pure-power at H' can be expressed as (50).

$$Q_{gt}^{H^*} = Q_{gt}^B \quad (49)$$

$$P_{gt}^{H'} = P_{gt}^H + k_g^R Q_{gt}^H - (k_g^R + k_g^{AB}) Q_g^B - b_g^R \quad (50)$$

Constraints (48) and (50) show that the pure-power $P_{gt}^{H'}$ can be expressed by the general form in (39), and the coefficients $a_g^j$, $b_g^j$ and $c_g^j$ can be easily extracted from (10), (48) and (50). This is similar to the case for the bypass-CHP unit. Further, by combining (14)-(17) and (39), $P_{gts}^{H'}$ can be expressed by (40). Finally, the ramping constraints for the LPCR-CHP unit can be formulated as (11)-(12) and (40).

### 4) MODE SWITCHING

By closing and opening the link valve, the LPCR-CHP unit can be switched between the ''zero LPC output'' mode and the ''non-zero LPC output'' mode. However, the frequent mode switching may affect the operational stability and safety of the CHP unit.

In this paper, the following constraints are employed to restrict the switching frequency. In these constraints, new continuous variables $w_{gt}^+$ and $w_{gt}^-$ are introduced, $I_{gt}^2$ and $I_{gt}^3$ represent whether the unit operates on lines B'C' and C'D,' respectively. Specifically, these constraints guarantee that if the operation region of the unit is switched from area ABCDE to lines B'C'-C'D' (i.e., the link valve is closed), the unit will operate on lines B'C'-C'D' and the link valve will keep closing for at least $T_g^+$ time intervals. Similarly, if the working region is switched back from lines B'C'-C'D' to area ABCDE (i.e., the link valve is opened), the unit will operate inside area ABCDE and the link valve will keep opening for at least $T_g^-$ time intervals. The allowable switching frequency can be adjusted by varying the values of $T_g^+$ and $T_g^-$, with larger values of $T_g^+$ and $T_g^-$ leading to lower switching frequency.

$$w_{gt}^+ \geq I_{gt}^2 + I_{gt}^3 - I_{g,t-1}^2 - I_{g,t-1}^3 \quad (51)$$

$$w_{gt}^- \geq I_{g,t-1}^2 + I_{g,t-1}^3 - I_{gt}^2 - I_{gt}^3 \quad (52)$$

$$w_{gt}^+ \geq 0,\ w_{gt}^- \geq 0 \quad (53)$$

$$\sum_{\tau=t-T_g^+ +1}^{t} w_{g\tau}^+ \leq I_{gt}^2 + I_{gt}^3 \quad (54)$$

$$\sum_{\tau=t-T_g^- +1}^{t} w_{g\tau}^- \leq 1 - I_{gt}^2 - I_{gt}^3 \quad (55)$$

## III. FORMULATION OF THE PROPOSED UNIT COMMITMENT MODEL

Based on the modelling of the operation of CHP units in Section II, a UC model incorporating the bypass and LPCR retrofit of CHP units is constructed in this section. The whole model is a mixed-integer linear optimization problem, which can be solved by off-the-shelf solvers, like Gurobi [29].

### A. OBJECTIVE FUNCTION

The proposed UC model aims to minimize the total operational cost of the CHP system:

$$\underset{\Omega}{\text{Min}} \sum_{t\in\mathcal{T}} \left( \begin{array}{l} \sum\limits_{g\in\mathcal{G}^C} C_{gt}^C + \sum\limits_{g\in\mathcal{G}^H} C_{gt}^H + \sum\limits_{g\in\mathcal{G}} C_g^U S_{gt}^U \\ + \sum\limits_{r\in\mathcal{R}} C^{RC} P_{rt}^{RC} \Delta t + C^{LS} P_t^{LS} \Delta t \end{array} \right) \tag{56}$$

where the 1st to 2nd terms evaluate the fuel costs of condensing units and CHP units, respectively, the 3rd term denotes the start-up cost of all thermal units, and the 4th to 5th terms define the penalty costs for wind power curtailment and load shedding, respectively.

### B. OPERATIONAL CONSTRAINTS

*Constraints on the unit commitment of thermal units:* these constraints involve the unit commitment status equations, see (57a), and the minimum on and off times, see (57b)-(57c), of all condensing and CHP units.

$$S_{gt}^U - S_{gt}^D = I_{gt}^O - I_{g,t-1}^O, \forall g, \forall t \tag{57a}$$

$$\sum_{\tau=t-T_g^U+1}^{t} S_{g\tau}^U \le I_{gt}^O, \forall g, \forall t \tag{57b}$$

$$\sum_{\tau=t-T_g^D+1}^{t} S_{g\tau}^D \le 1 - I_{gt}^O, \forall g, \forall t \tag{57c}$$

2) *Constraints on condensing units:* these constraints involve the fuel cost function (58), the range of power output, see (59)-(60), the capacities of up- and down-reserves, see (61)-(62), and the ramping limits, see (63)-(64).

$$C_{gt}^C = a_g P_{gt}^{Con} + b_g I_{gt}^O, \forall g \in \mathcal{G}^C, \forall t \tag{58}$$

$$P_{gt}^{Con} + R_{gt}^+ \le I_{gt}^O \overline{P}_g, \forall g \in \mathcal{G}^C, \forall t \tag{59}$$

$$P_{gt}^{Con} - R_{gt}^- \ge I_{gt}^O \underline{P}_g, \forall g \in \mathcal{G}^C, \forall t \tag{60}$$

$$0 \le R_{gt}^+ \le \overline{R}_g^+, \forall g \in \mathcal{G}^C, \forall t \tag{61}$$

$$0 \le R_{gt}^- \le \overline{R}_g^-, \forall g \in \mathcal{G}^C, \forall t \tag{62}$$

$$P_{gt}^{Con} - P_{g,t-1}^{Con} \le I_{g,t-1}^O O_g^+ \Delta t + S_{gt}^U \max(O_g^+ \Delta t, \underline{P}_g), \forall g \in \mathcal{G}^C, \forall t \tag{63}$$

$$P_{g,t-1}^{Con} - P_{gt}^{Con} \le I_{gt}^O O_g^- \Delta t + S_{gt}^D \max(O_g^- \Delta t, \underline{P}_g), \forall g \in \mathcal{G}^C, \forall t \tag{64}$$

3) *Constraints on CHP units without retrofit:* see Section II-A.

$$(1) - (13), \forall g \in \mathcal{G}^{HN}, \forall t \tag{65}$$

4) *Constraints on CHP units with bypass:* see Section II-B.

$$(14) - (27), (11) - (13), (40), \forall g \in \mathcal{G}^{HB}, \forall t \tag{66}$$

5) *Constraints on CHP units with LPCR:* see Section II-C.

$$(14) - (18), (41) - (45), (11) - (13), (40), (51) - (55), \forall g \in \mathcal{G}^{HL}, \forall t \tag{67}$$

6) *Constraints on the output of wind farms:*

$$P_{rt}^{RO} + P_{rt}^{RC} = P_{rt}^{RA}, \forall r, \forall t \tag{68}$$

$$P_{rt}^{RC} \ge 0, P_{rt}^{RO} \ge 0, \forall r, \forall t \tag{69}$$

7) *System-wide power balance constraints:*

$$\sum\nolimits_{g\in\mathcal{G}^C} P_{gt}^{Con} + \sum\nolimits_{g\in\mathcal{G}^H} P_{gt}^H + \sum\nolimits_{r\in\mathcal{R}} P_{rt}^{RO} = P_t^{PL} - P_t^{LS}, \forall t \tag{70}$$

$$P_t^{LS} \ge 0, \forall t \tag{71}$$

8) *Zonal heat-balance constraints:* the heating demand is satisfied separately within each heating district.

$$\sum\nolimits_{g\in\mathcal{G}_k^H} Q_{gt}^H = Q_{tk}^L, \forall t, \forall k \tag{72}$$

9) *System-wide upward and downward reserve requirements:*

$$\sum\nolimits_{g\in\mathcal{G}} R_{gt}^+ \ge \zeta^{L+} P_t^L + \zeta^{R+} \sum\nolimits_{r\in\mathcal{R}} P_{rt}^{RO}, \forall t \tag{73}$$

$$\sum\nolimits_{g\in\mathcal{G}} R_{gt}^- \ge \zeta^{L-} P_t^L + \zeta^{R-} \sum\nolimits_{r\in\mathcal{R}} P_{rt}^{RO}, \forall t \tag{74}$$

10) *Other constraints:* Other constraints include the DC power flow constraints, which employ the form as in [21].

*Remark 1:* The proposed UC model can be readily extended to include both heat storage and electric boilers. To achieve the extension, the operational modelling of heat storage and electric boilers needs to be integrated into the UC scheduling, and the modelling methods for these devices have received wide research (see, e.g., [21], [30], [31]). Meanwhile, the power and heat-balance constraints need to be modified to account for the inflow/outflow heat from the heat storage and the power consumption/heat generation from the electric boiler (see [30], [31]).

*Remark 2:* The utilization of LPCR and bypass retrofit may increase the computational burden of the UC model due to the introduced sub-regions and auxiliary variables. Since this paper focuses on the tractability of the UC formulation and the effectiveness of the model in utilizing the LPCR and bypass retrofit, the improvement of the computational performance is left for next work. One potential method is the heuristics for the warm-start of binary variables [32].

## IV. CASE STUDIES

A test system is constructed to study the performance of the proposed UC model. All numerical cases are coded in MATLAB via YALMIP on a laptop with Intel Core i5-1240P CPU and 16GB RAM, and all the optimization problems are solved by Gurobi with the tolerance gap of mixed-integer programming set at 0.01%.

### A. CASE SETTINGS

The structure of the test system can be found in [3]. In this paper, the system consists of four thermal units (CHP1-CHP2 and G1-G2) and a wind farm. The four thermal units have the same technical and cost parameters, but G1-G2 only works

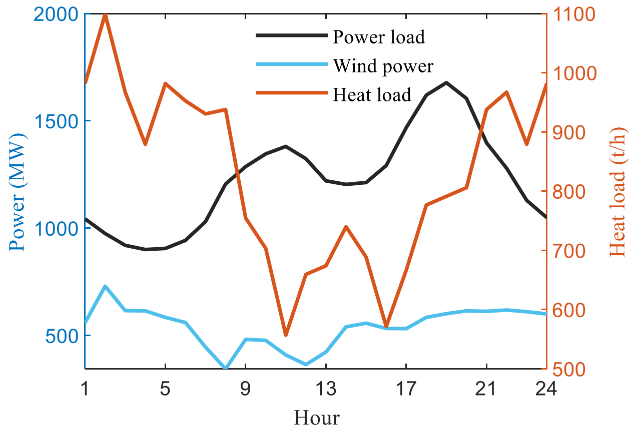


**FIGURE 7.** The profiles of power load, heat load and available wind power.

in full-condensing state while CHP1-CHP2 supplies both electricity and heat.

The safe operation regions of CHP1 and CHP2 can be seen in Fig. 2, Fig. 4 and Fig. 6, when they have no flexibility retrofit, the bypass retrofit and LPCR retrofit, respectively. For the CHP units with LPCR retrofit, $T_g^+$ and $T_g^-$ are set to 3 h. The other parameters of the CHP units are listed in Table 1. Specifically, the cost coefficients are determined based on the coal consumption parameters from [33] and the coal price of 700 CNY/t according to National Bureau of Statistics; the start-up cost is from [34]; other technical parameters including the ramping limits are referred to [35], [36]. The parameters of G1-G2 can be also found in Table 1. Note that the output ranges of G1-G2 are represented by the line AE in Fig. 2.

The profiles of hourly total system power and heat load as well as available wind power are shown in Fig. 7. There are two heating districts with equal heat demands, with district I (bus 3) served by CHP1 and district II (bus 6) served by CHP2. The total power load is distributed equally at two districts. As for the reserve factors, $\zeta^{L+}$ and $\zeta^{L-}$ are set to 5%, and $\zeta_r^{R+} = \zeta_r^{R-} = 20\%$ [36]. The penalty price for the wind curtailment and load shedding are 150 CNY/MWh and 7500 CNY/MWh, respectively [22], [37]. The dispatch horizon consists of 24 hours.

**TABLE 1.** Some parameters of units CHP1-CHP2.

| | |
|---|---|
| $T_g^U/T_g^D$ (h) | 8 |
| $O_g^+/O_g^-$ (MW/h) | 89.1 |
| $\overline{R}_g^+/\overline{R}_g^-$ (MW) | 89.1 |
| $a_g$ (CNY/MWh) | 188.5 |
| $b_g$ (CNY/h) | 685.8 |
| $C_g^U$ ($10^4$ CNY) | 5.7 |

## B. EFFECTIVENESS OF THE PROPOSED UC MODEL

To test whether the proposed UC model can utilize the flexibility from the retrofit of CHP units to benefit system operation, the following scenarios are studied:

1) S1: all CHP units have no flexibility retrofit.
2) S2: all CHP units complete the bypass retrofit.
3) S3: all CHP units complete the LPCR retrofit.

In scenarios S1-S3, CHP units have different safe operation regions, and the proposed UC model is solved under each of the scenarios. The solution time of the model is within a few seconds.

Table 2 compares the total fuel and system costs as well as the wind curtailment rates in scenarios S1-S3. It can be seen that the LPCR and bypass retrofit can both improve the operational economy and reduce the wind curtailment, but the benefits from the bypass retrofit are much more obvious. Under the LPCR retrofit, the amount of wind curtailment is reduced by 20.45%, while such percentage is 81.94% under the bypass retrofit.

**TABLE 2.** Total fuel and system costs as well as wind curtailment in scenarios S1-S3.

| Scenarios | S1 | S2 | S3 |
|---|---|---|---|
| Total fuel cost (million CNY) | 4.90 | 4.78 | 4.63 |
| Total operational cost (million CNY) | 5.20 | 5.02 | 4.68 |
| Wind curtailment (GWh) | 2.00 | 1.59 | 0.36 |
| Wind curtailment rate (%) | 15.36 | 12.22 | 2.77 |

To explain the reduced system cost and wind curtailment by flexibility retrofit, the profiles of hourly wind curtailment in S1-S3 are compared in Fig. 8, the profiles of the hourly power output of thermal units in S1-S3 are plotted in Fig. 9, the operating modes of the link valves in CHP1 and CHP2 are shown in Fig. 10.

It is found from Fig. 8 that compared to S1, the wind curtailment is lower in S2 during hours 1-6 and 23-24. In these time intervals, the heat load and available wind power are both high but the system load is low (see Fig. 7), so the accommodation of wind power needs to be balanced by the reduction in the power output of thermal units. However, under the constraints of heat-power coupling, the CHP units without retrofit have to maintain a high level of power output in order to meet the heat load (see Fig. 9). This causes the curtailment of wind power.

By comparison, the CHP units with LPCR retrofit can choose to close the link valve during the periods with high heat load (see CHP2 in Fig. 10), so the total power output of CHP units can be reduced during hours 1-6 and 23-24 (see Fig. 9). Thus, more wind power can be accommodated in S2. To present this point more clearly, the heat-power output of CHP2 in S1-S2 during hours 1-6 are plotted in Fig. 11 (a). It can be seen that CHP2 can have lower power output in S2. Besides, the increased utilization of wind power means decreased power output of thermal units and lower

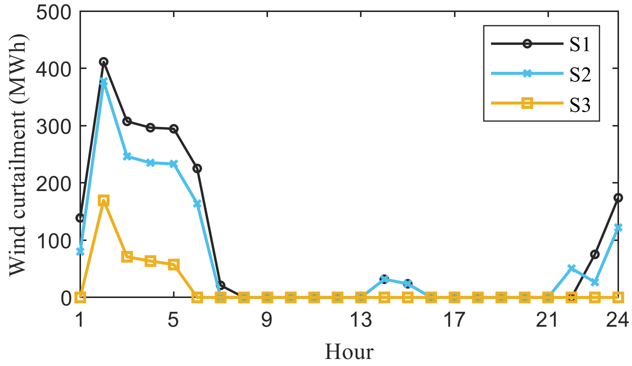


**FIGURE 8.** Hourly wind power curtailment in scenarios S1-S3.

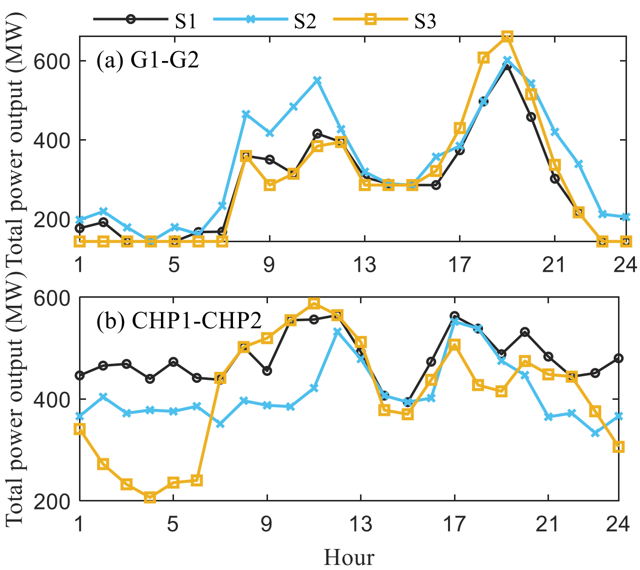


**FIGURE 9.** Total power output of G1-G3 and total power output of CHP1-CHP2 in scenarios S1-S3.

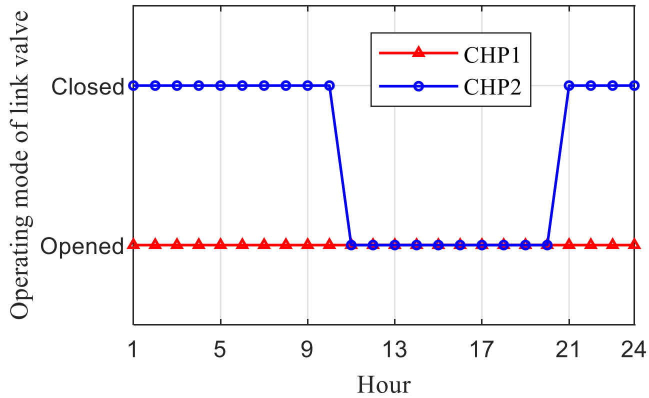


**FIGURE 10.** Operating modes of the link valves in CHP1-CHP2 in scenarios S2.

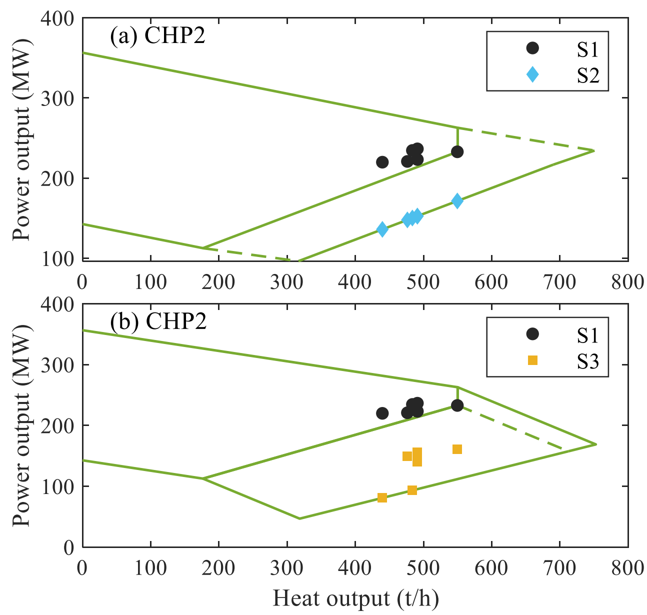


**FIGURE 11.** Heat-power output of CHP2 during hours 1-6 in different scenarios.

consumption of fossil fuel, so the fuel and system cost can be reduced.

Fig. 8 also shows that the bypass retrofit in S3 yields much lower wind curtailment compared to the LPCR retrofit in S2. This is mainly because the CHP units can have lower power output in S3 during hours 1-6 and 23-24 (see Fig. 9). Actually, the bypass retrofit can produce more flexible operation region for CHP units, so the power output of CHP units under the high heat load is allowed to be lower. This point is also reflected in Fig. 11. Besides, the LPCR-CHP units cannot provide reserves when the link valve is closed, so the condensing units G1-G2 have to be online to provide reserves in hours 1-6, see Fig. 9(a). By comparison, bypass-CHP units still have reserve capabilities, thus G1-G2 are allowed to be offline to have zero power output in hours 1-6. This is another reason why the room to accommodate wind power is larger in S3.

The above results also reveal that the proposed UC model is capable of utilizing the flexibility provided by the bypass and LPCR retrofit to facilitate wind integration and reduce operational cost.

### *C. DIFFERENT MODELLING ON THE RAMPING CONSTRAINTS OF CHP UNITS*

In this paper, the ramping constraints of CHP units are modelled by converting the operating state H into the corresponding pure-power state H.' In the literature, there is an alternative formulation for the ramping capacities of CHP units (see, e.g., [22]):

$$P^H_{gt} - P^H_{g,t-1} \le I_{g,t-1} O^+_g \Delta t + S^U_{gt} \max\left(O^+_g \Delta t, P^E_{gt}\right) \quad (75a)$$

$$P^H_{gt} - P^H_{g,t-1} \le I_{g,t} O^-_g \Delta t + S^D_{gt} \max\left(O^-_g \Delta t, P^E_{gt}\right) \quad (75b)$$

In (75), only the ramping in the power output of CHP units is restricted, neglecting the coupled relationship between the power and heat output. For the 6-bus system, the UC problems considering the proposed constraints and the alternative in (75) are both solved, and the results are compared in terms of the ramping safety of CHP units.

Take CHP1 as an example, its power and heat output are converted into the corresponding pure-power, and the change in the pure-power represents the ramping in the main steam flow of the unit. That is, if the change rate of the pure-power exceeds the up- or down-limit, the ramping of the main steam flow is beyond the safe range.

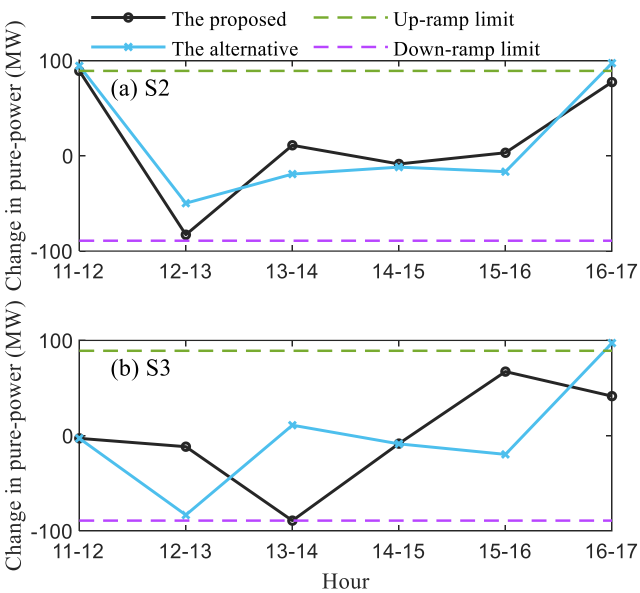


**FIGURE 12.** Change in the pure-power of CHP1 during every two consecutive hours.

For CHP1, its change rates in the pure power from hour 11 to hour 17 are plotted in Fig. 12. Clearly, when the alternative constraints in (75) are employed, the operation of CHP1 exceeds the up-ramp limit from hour 11 to hour 12 and hour 16 to hour 17 in scenario S2; and in scenario S3, CHP1 fails to satisfy the up-ramp safety from hour 16 to hour 17. To be contrary, the ramping safety of CHP1 can be satisfied when the proposed ramping constraints take effect. Actually, the results of the UC optimization show that all CHP units can operate within safe ramping ranges under the proposed ramping constraints.

### *D. SENSITIVITY ANALYSIS*

To test if the flexibility retrofit can benefit system operation under various conditions, sensitivity analysis is conducted for different levels of fuel cost, reserve capacities and wind power variability:

1) the fuel cost coefficient $a_g$ of each CHP unit is changed by the percentage ranging from -40% to 40%.

2) the reserve capacities of each CHP unit are changed by the percentage ranging from -60% to 60%.

3) To simulate different wind power variability, 60 different wind power profiles are drawn from the actual data in a provincial system in China.

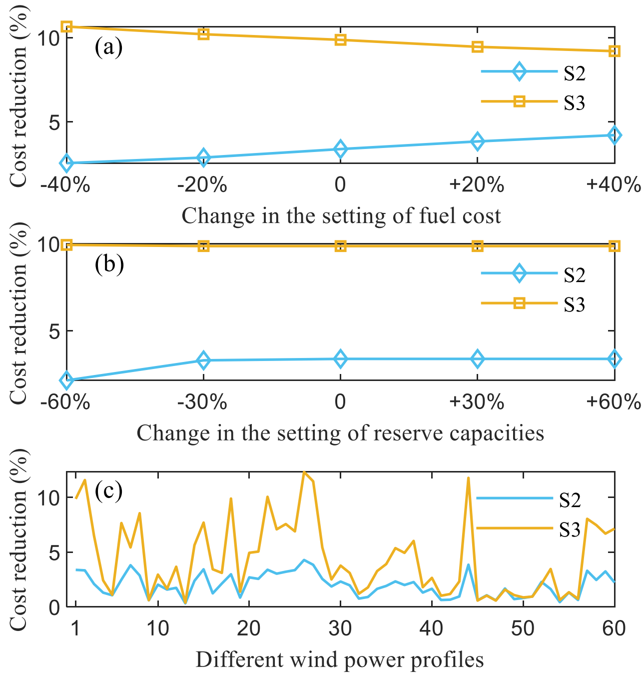


**FIGURE 13.** The reduction in total operational cost when scenario S2/S3 is compared to scenario S1.

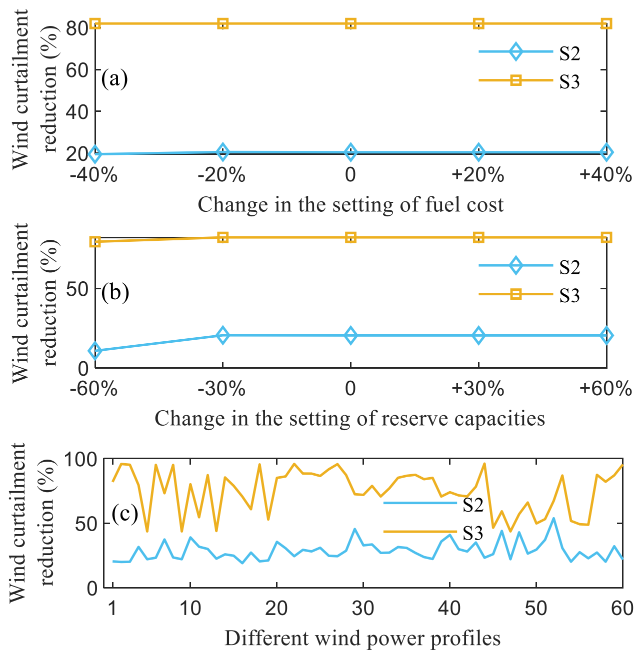


**FIGURE 14.** The reduction in total wind curtailment when scenario S2/S3 is compared to scenario S1.

Under each of the above conditions, the proposed UC model is solved for each of the scenarios S1-S3. The operational cost and wind curtailment for S2 and S3 are compared to those for S1, and the comparison results are shown in Fig. 13 and Fig. 14. It can be seen that, compared to the "no-retrofit" in S1, the LPCR retrofit in S2 yields reduced operational cost and wind curtailment under various conditions. Similar observations are also found for the bypass retrofit in S3.

The simulation results also reveal that the benefit of LPCR retrofit in cost reduction is larger under higher setting of fuel cost, but such trend is converse with that for bypass retrofit. And the cost reduction for LPCR retrofit may not be obvious under very low reserve capacities. Besides, compared to fuel cost and reserve capacities, the wind power profile has larger impact on the benefits of flexibility retrofit. Among various wind power profiles, the maximum reduction in operational cost is 4.29% for S2 and 16.21% for S3, and the maximum reduction in wind curtailment achieves 53.84% for S2 and 96.15% for S3.

## V. CONCLUSION

This paper presents a novel UC model which explicitly accounts for the bypass and LPCR retrofit of CHP units. In this model, the constraints for the safe operation region, fuel cost, ramping capability, reserve capacities and mode switching of CHP units are thoroughly constructed in a tractable way. The proposed model fills the gap in the literature, which has not yet integrated the bypass and LPCR retrofit of CHP units into the UC problem. Based on the case studies on a test system, some valuable observations are drawn:

- The proposed UC model is capable of utilizing the flexibility from bypass and LPCR retrofit to accommodate more wind power and reduce the operational cost. For the LPCR retrofit, the reduction in the operational cost and wind curtailment can reach 3.46% and 20.45%, respectively. For the bypass retrofit, these two percentages can reach 10.00% and 81.94%, respectively.
- Compared to the LPCR retrofit, the bypass retrofit enables larger reduction in both wind curtailment and operational cost. This is mainly due to the more flexible operational region and reserve capability from the bypass retrofit.
- In addition, it is found that the proposed ramping constraints enable the CHP units to work within safe ramping ranges, while the conventional ramping constraints fail to satisfy the ramping safety.

The main advantage of the proposed UC model is that it can utilize the flexibility of bypass and LPCR retrofit in a tractable and effective way. Such flexibility facilitates the wind integration and improves the operational economy of the CHP system. Besides, this UC model is capable of describing the accurate ramping constraints of CHP units, which are rarely considered in the existing UC models.

The limitations of the current UC model and the future work are also discussed as follows.

- The inclusion of flexibility retrofit may increase the computational burden of the UC model. The heuristics for warm-start will be studied in the next work to improve the scalability of the model (e.g., see [32]).
- The carbon-emission of thermal units is not the research focus of this paper, but the future work will attempt to integrate it into the UC model [38].

## REFERENCES

[1] W. Zheng, Y. Zhang, J. Xia, and Y. Jiang, "Cleaner heating in northern China: Potentials and regional balances," *Resour., Conservation Recycling*, vol. 160, Sep. 2020, Art. no. 104897, doi: 10.1016/j.resconrec.2020.104897.

[2] J. Beiron, L. Göransson, F. Normann, and F. Johnsson, "A multiple system level modeling approach to coupled energy markets: Incentives for combined heat and power generation at the plant, city and regional energy system levels," *Energy*, vol. 254, Sep. 2022, Art. no. 124337, doi: 10.1016/j.energy.2022.124337.

[3] T. Jin, X. Chen, J. Wen, Q. Wu, L. Bai, Y. Liu, and Y. Cao, "Improved ramping and reserve modeling of combined heat and power in integrated energy systems for better renewable integration," *IEEE Trans. Sustain. Energy*, vol. 13, no. 2, pp. 683–692, Apr. 2022, doi: 10.1109/TSTE.2021.3127245.

[4] X. Guo, S. Lou, Z. Chen, Y. Wu, and Y. Wang, "Stochastic optimal scheduling considering reserve characteristics of retrofitted combined heat and power plants," *Int. J. Electr. Power Energy Syst.*, vol. 140, Sep. 2022, Art. no. 108051, doi: 10.1016/j.ijepes.2022.108051.

[5] A. F. Heidari, A. Masoumzadeh, M. Vrakopoulou, and T. Alpcan, "Planning for inertia and resource adequacy in a renewable-rich power system," in *Proc. IEEE PES Innov. Smart Grid Technol. Asia (ISGT Asia)*, Nov. 2023, pp. 1–5, doi: 10.1109/isgtasia54891.2023.10372655.

[6] *Inner Mongolia Renewable Energy Development Report 2023*, Inner Mongolia Energy Bur., China Renew. Energy Eng. Inst., Econ. Press, Beijing, China, 2023.

[7] D. Zhang, Y. Hu, and Y. Gao, "Flexibility improvement of CHP unit for wind power accommodation," *J. Modern Power Syst. Clean Energy*, vol. 10, no. 3, pp. 731–742, May 2022, doi: 10.35833/MPCE.2020.000630.

[8] M. Foroughi, A. Pasban, M. Moeini-Aghtaie, and A. Fayaz-Heidari, "A bi-level model for optimal bidding of a multi-carrier technical virtual power plant in energy markets," *Int. J. Electr. Power Energy Syst.*, vol. 125, Feb. 2021, Art. no. 106397, doi: 10.1016/j.ijepes.2020.106397.

[9] K. Zhang, M. Liu, Y. Zhao, H. Yan, and J. Yan, "Design and performance evaluation of a new thermal energy storage system integrated within a coal-fired power plant," *J. Energy Storage*, vol. 50, Jun. 2022, Art. no. 104335.

[10] K. Zhang, M. Liu, Y. Zhao, S. Zhang, H. Yan, and J. Yan, "Thermo-economic optimization of the thermal energy storage system extracting heat from the reheat steam for coal-fired power plants," *Appl. Thermal Eng.*, vol. 215, Oct. 2022, Art. no. 119008.

[11] X. Huang, Z. Xu, Y. Sun, Y. Xue, Z. Wang, Z. Liu, Z. Li, and W. Ni, "Heat and power load dispatching considering energy storage of district heating system and electric boilers," *J. Modern Power Syst. Clean Energy*, vol. 6, no. 5, pp. 992–1003, Sep. 2018.

[12] M. Liu, S. Wang, Y. Zhao, H. Tang, and J. Yan, "Heat–power decoupling technologies for coal-fired CHP plants: Operation flexibility and thermodynamic performance," *Energy*, vol. 188, Dec. 2019, Art. no. 116074, doi: 10.1016/j.energy.2019.116074.

[13] L. Cao, Z. Wang, T. Pan, E. Dong, P. Hu, M. Liu, and T. Ma, "Analysis on wind power accommodation ability and coal consumption of heat–power decoupling technologies for CHP units," *Energy*, vol. 231, Sep. 2021, Art. no. 120833, doi: 10.1016/j.energy.2021.120833.

[14] Q. Hu, K. Wang, L. Zhang, L. Zhou, R. Chen, S. Wang, Y. Zhang, and G. Li, "Theoretical investigation on heat-electricity decoupling technology of low-pressure steam turbine renovation for CHPs," *IOP Conf. Ser., Earth Environ. Sci.*, vol. 227, Mar. 2019, Art. no. 042043.

[15] J. Liu and L. Zhu, "Application research on zero output of double low pressure cylinder of 600MW unit," in *Proc. E3S Web Conf.* Les Ulis, France: EDP Sciences, 2023, p. 02017.

[16] R. Yan, J. Wang, S. Huo, J. Zhang, S. Tang, and M. Yang, "Comparative study for four technologies on flexibility improvement and renewable energy accommodation of combined heat and power system," *Energy*, vol. 263, Jan. 2023, Art. no. 126056, doi: 10.1016/j.energy.2022.126056.

[17] C. Chen, Y. Zhang, Z. Ge, X. Du, and E. Saad ELSihy, "Comparative study on flexibility enhancement of combined heat and power for wind power accommodation," *Appl. Thermal Eng.*, vol. 235, Nov. 2023, Art. no. 121287, doi: 10.1016/j.applthermaleng.2023.121287.

[18] C. Wang and J. Song, "Performance assessment of the novel coal-fired combined heat and power plant integrating with flexibility renovations," *Energy*, vol. 263, Jan. 2023, Art. no. 125886, doi: 10.1016/j.energy.2022.125886.

[19] X. Chen, C. Kang, M. O'Malley, Q. Xia, J. Bai, C. Liu, R. Sun, W. Wang, and H. Li, "Increasing the flexibility of combined heat and power for wind power integration in China: Modeling and implications," *IEEE Trans. Power Syst.*, vol. 30, no. 4, pp. 1848–1857, Jul. 2015, doi: 10.1109/TPWRS.2014.2356723.

[20] X. Chen, M. B. McElroy, and C. Kang, "Integrated energy systems for higher wind penetration in China: Formulation, implementation, and impacts," *IEEE Trans. Power Syst.*, vol. 33, no. 2, pp. 1309–1319, Mar. 2018, doi: 10.1109/TPWRS.2017.2736943.

[21] B. Liu, J. Li, S. Zhang, M. Gao, H. Ma, G. Li, and C. Gu, "Economic dispatch of combined heat and power energy systems using electric boiler to accommodate wind power," *IEEE Access*, vol. 8, pp. 41288–41297, 2020, doi: 10.1109/ACCESS.2020.2968583.

[22] T. Zhao, Y. Zheng, and G. Li, "Integrated unit commitment and economic dispatch of combined heat and power system considering heat-power decoupling retrofit of CHP unit," *Int. J. Electr. Power Energy Syst.*, vol. 143, Dec. 2022, Art. no. 108498, doi: 10.1016/j.ijepes.2022.108498.

[23] J. Wu, "Flexibility transformation technology research and strategy analysis of thermal power units in Northeast China," *Heilongjiang Electr. Power*, vol. 42, no. 5, pp. 443–446, Oct. 2020, doi: 10.13625/j.cnki.hljep.2020.05.014.

[24] Z. Wang, L. Cao, E. Dong, P. Hu, M. Liu, and T. Ma, "Improving wind power accommodation of combined heat and power plant based on bypass system," *Acta Energiae Solaris Sin.*, vol. 42, no. 1, pp. 317–323, Jan. 2021, doi: 10.19912/j.0254-0096.tynxb.2019-0538.

[25] C. Liu, L. Geng, H. Wang, H. Miao, Z. Shang, and L. Zeng, "Control strategy in transformation of high and low pressure bypass combined heat supply," *Therm. Power Gener.*, vol. 49, no. 11, pp. 126–132, Mar. 2020, doi: 10.19666/j.rlfd.202002016.

[26] W. Dong, P. Si, W. M. Wang, and P. Zhang, "Analysis of the influence of HP-IP bypass heat supply reformation on unit's peak shaving capability," *J. Eng. Therm. Energy Power*, vol. 38, no. 8, pp. 169–175, Aug. 2023, doi: 10.16146/j.cnki.rndlgc.2023.08.021.

[27] Y. Gao, Y. Hu, D. Zeng, J. Liu, and F. Chen, "Modeling and control of a combined heat and power unit with two-stage bypass," *Energies*, vol. 11, no. 6, p. 1395, May 2018, doi: 10.3390/en11061395.

[28] Y. Gao, D. Zeng, L. Zhang, Y. Hu, and Z. Xie, "Research on modeling and deep peak regulation control of a combined heat and power unit," *IEEE Access*, vol. 8, pp. 91546–91557, 2020, doi: 10.1109/ACCESS.2020.2993279.

[29] (2023). *Gurobi Optimizer Reference Manual*. [Online]. Available: https://www.gurobi.com

[30] J. Liu, A. Wang, C. Song, R. Tao, and X. Wang, "Cooperative operation for integrated multi-energy system considering transmission losses," *IEEE Access*, vol. 8, pp. 96934–96945, 2020, doi: 10.1109/ACCESS.2020.2996913.

[31] S. Zhu, E. Wang, S. Han, and H. Ji, "Optimal scheduling of combined heat and power systems integrating hydropower-wind-photovoltaic-thermal-battery considering carbon trading," *IEEE Access*, vol. 12, pp. 98393–98406, 2024, doi: 10.1109/ACCESS.2024.3429399.

[32] J. Ling, L. Zhang, G. Geng, and Q. Jiang, "Feasible-enabled integer variable warm start strategy for security-constrained unit commitment," *Int. J. Electr. Power Energy Syst.*, vol. 160, Sep. 2024, Art. no. 110137, doi: 10.1016/j.ijepes.2024.110137.

[33] Y. Zhang, Q. Lyu, Y. Li, N. Zhang, H. Wang, and H. Sun, "Analysis on operation flexibility of combined heat and power plant with four improved power-heat decoupling schemes," *Autom. Electr. Power Syst.*, vol. 44, no. 2, pp. 164–172, 2020, doi: 10.7500/AEPS20190509006.

[34] Z. Zhao and Y. Hao, "Cost optimization of renewable energy accommodation system based on flexibility renovation of thermal power units," *Modern Electr. Power*, vol. 41, no. 2, pp. 326–334, 2024, doi: 10.19725/j.cnki.1007-2322.2022.0246.

[35] P. J. Ramírez, D. Papadaskalopoulos, and G. Strbac, "Co-optimization of generation expansion planning and electric vehicles flexibility," *IEEE Trans. Smart Grid*, vol. 7, no. 3, pp. 1609–1619, May 2016, doi: 10.1109/TSG.2015.2506003.

[36] X. Chen, J. Lv, M. B. McElroy, X. Han, C. P. Nielsen, and J. Wen, "Power system capacity expansion under higher penetration of renewables considering flexibility constraints and low carbon policies," *IEEE Trans. Power Syst.*, vol. 33, no. 6, pp. 6240–6253, Nov. 2018, doi: 10.1109/TPWRS.2018.2827003.

[37] L. You, H. Ma, T. K. Saha, and G. Liu, "Risk-based contingency-constrained optimal power flow with adjustable uncertainty set of wind power," *IEEE Trans. Ind. Informat.*, vol. 18, no. 2, pp. 996–1008, Feb. 2022, doi: 10.1109/TII.2021.3076801.

[38] A. U. Rehman, G. Hafeez, F. R. Albogamy, Z. Wadud, F. Ali, I. Khan, G. Rukh, and S. Khan, "An efficient energy management in smart grid considering demand response program and renewable energy sources," *IEEE Access*, vol. 9, pp. 148821–148844, 2021, doi: 10.1109/ACCESS.2021.3124557.

**LEI YOU** received the B.Eng. degree from Liaoning University, Shenyang, China, in 2015, the master's degree from South China University of Technology, Guangzhou, China, in 2018, and the Ph.D. degree from The University of Queensland, Brisbane, QLD, Australia, in 2022, all in electrical engineering. He is currently conducting his postdoctoral research with Guangdong Electric Power Design Institute Company Ltd., China. His research interests include power system security, optimization, and renewable energy integration.

**XIAOMING JIN** was born in Loudi, Hunan, China, in 1963. He received the B.Eng. degree in China. He is currently the Deputy Chief Engineer of Guangdong Electric Power Design Institute Company Ltd., China. His research interests include power system planning and DC transmission.

**YUN LIU** was born in Xuancheng, Anhui, China, in 1983. She received the master's degree in Wuhan, China. She is currently the Vice-General Manager of the Energy Consulting and Planning Institute, Guangdong Electric Power Design Institute Company Ltd., China. Her research interests include power system planning and renewable energy integration.